arXiv:1610.02962v1 [stat.ML] 10 Oct 2016

LOW-RANK APPROXIMATION AND DYNAMIC MODE DECOMPOSITION

P. HÉAS* AND C. HERZET*

Abstract. Dynamic Mode Decomposition (DMD) has emerged as a powerful tool for analyzing the dynamics of non-linear systems from experimental datasets. Recently, several attempts have extended DMD to the context of low-rank approximations. This extension is of particular interest for reduced-order modeling in various applicative domains, *e.g.*, for climate prediction, to study molecular dynamics or micro-electromechanical devices. This low-rank extension takes the form of a nonconvex optimization problem. To the best of our knowledge, only sub-optimal algorithms have been proposed in the literature to compute the solution of this problem. In this paper, we prove that there exists a closed-form optimal solution to this problem and design an effective algorithm to compute it based on Singular Value Decomposition (SVD). Based on this solution, we then propose efficient procedures for reduced-order modeling and for the identification of the the low-rank DMD modes and amplitudes. Experiments illustrates the gain in performance of the proposed algorithm compared to state-of-the-art techniques.

1. Introduction.

In many fields of Sciences, one is interested in studying the spatio-temporal evolution of a state variable characterized by a partial differential equation. Numerical discretization in space and time leads to a high dimensional system of equations of the form:

$$\begin{cases} x_t = f_t(x_{t-1}), \\ x_1 = \theta, \end{cases} \tag{1.1}$$

where each element of the sequence of state variables $\{x_t\}_t$ belongs to $\mathbb{R}^n$, $f_t : \mathbb{R}^n \to \mathbb{R}^n$ with the initial condition $\theta \in \mathbb{R}^n$. Because (1.1) may correspond to a very high-dimensional system in some applications, computing a trajectory $\{x_t\}_t$ given an initial condition θ may lead to a heavy computational load, which may prohibit the direct use of the original high-dimensional system.

The context of uncertainty quantification provides an appealing example. Assume we are interested in characterizing the distribution of random trajectories generated by (1.1) with respect to the distribution of the initial condition. A straightforward approach would be to sample the initial condition and run the high-dimensional system. However, in many applicative contexts, it is impossible to generate enough trajectories to make accurate approximations with Monte-Carlo techniques.

As a response to this computational bottleneck, reduced-order models aim to approximate the trajectories of the system for a range of regimes determined by a set of initial conditions [5]. A common approach is to assume that the trajectories of interest are well approximated in a sub-space of $\mathbb{R}^n$. In this spirit, many tractable low-rank approximations of high-dimensional systems have been proposed in the literature, the most familiar being proper orthogonal decomposition (POD) [10], balanced truncation [1], Taylor expansions [8] or reduced-basis techniques [22]. Approximation of second-order nonlinear operators has recently been proposed in [20]. Other popular sub-space methods, such as linear inverse modeling (LIM) [21], principal oscillating patterns (POP) [9], or more recently, dynamic mode decomposition (DMD) [24, 27, 26] or low-rank DMD [4, 13] are known as Koopman operator approximations.

*INRIA Centre Rennes - Bretagne Atlantique, campus universitaire de Beaulieu, 35042 Rennes, France (patrick.heas@inria.fr, cedric.herzet@inria.fr)

On the other hand, besides the reduced modeling context, algorithms identifying DMD parameters have gained popularity because this decomposition reveals features of the dynamics, which are relevant for the analysis of experimental data [24, 27, 26]. However, in many situations, it is not trivial to identify accurately these parameters. This difficulty arises in particular when the data to be analysed is corrupted by noise. To deal with such situations, authors in [4, 13] have proposed algorithms to identify the dominant parameter of DMD by introducing a low-rank version of the DMD approximation.

In this paper, we consider a nonintrusive setting where system (1.1) is a black-box. In other words, we assume that we do not know the exact form of f_t in (1.1) and we only have access to a set of representative trajectories $\{x_t^i\}_{t,i}$, $i = 1, ..., N$, $t = 1, ..., T$ so-called *snapshots*, obtained by running the high-dimensional system for N different initial conditions. Moreover, we focus on the problem of low-rank DMD approximation studied in [4, 13]. In a nutshell, these studies provide a procedure for determining a matrix $\hat{A}_k$ of rank $k \ll n$, which substitutes function f_t in (1.1), *i.e.*,

$$\begin{cases} \tilde{x}_t = \hat{A}_k \tilde{x}_{t-1}, \\ \tilde{x}_1 = \theta, \end{cases} \tag{1.2}$$

and generates the approximations $\tilde{x}_t \in \mathbb{R}^n$ with a low computational effort. Matrix $\hat{A}_k$ targets the solution of the following nonconvex optimization problem, which we will refer to as the *low-rank DMD approximation problem*

$$A_k^\star = \underset{A:\mathrm{rank}(A)\leq k}{\arg\min} \sum_{t,i} \|x_t^i - A x_{t-1}^i\|_2^2, \tag{1.3}$$

where $\|\cdot\|_2$ denotes the ℓ_2-norm. Note that in the case $k \geq N(T-1)$, (1.3) becomes a nonconstrained least-square problem. The solution is in this case simply obtained by singular value decomposition (SVD) [26]. In what follows, we will focus on the more involved situation where $k < N(T-1)$.

Given the solution $A_k^\star$, and its (at most) k non-zero eigenvalues $\lambda_i \in \mathbb{C}$, $i = 1, \cdots, k$ and associated eigenvectors $\phi_i \in \mathbb{C}^n$, $i = 1, \cdots, k$, one can then compute trajectories of (1.2) by setting $\hat{A}_k = A_k^\star$ and using the reduced-order model

$$\tilde{x}_t = \sum_{i=1}^{k} \nu_{i,t} \phi_i, \tag{1.4}$$

$$\nu_{i,t} = \lambda_i^{t-1} \phi_i^* \tilde{x}_1. \tag{1.5}$$

In what follows, we will we refer to the parameters ϕ_i and $\nu_{i,t} \in \mathbb{C}$ as the *i-th low-rank DMD mode and amplitude* at time t. Alternatively, to compute trajectories of (1.2), we can build a reduced-order model taking the form of a k-dimensional recursion

$$\begin{cases} z_t = Q^* P z_{t-1}, \\ z_1 = P^* \tilde{x}_1, \end{cases} \tag{1.6}$$

where $P = W_{A_k^\star}$ and $Q = \Sigma_{A_k^\star} V_{A_k^\star}^*$. By multiplying both sides by matrix P, we then obtain the sought low-rank approximations $\tilde{x}_t = P z_t$. We remark that the overall complexity necessary to compute a trajectory with the original model (1.1) scales in $\mathcal{O}(n^2 T)$. In contrast, the reduced-order model (1.4) - (1.5) or (a diagonalized version

of) recursion (1.6) implies a complexity of $\mathcal{O}(k(n+T))$, scaling linearly with the ambient dimension.

At this point, let us mention that beyond the reduced modeling context discussed above, there has been a resurgence of interest for low-rank solutions of linear matrix equations in noise-free [7, 23] or noisy [14, 15, 12] settings. This class of problems is very large and includes in particular problem (1.3). Problems in this class are generally nonconvex and do not admit explicit solutions. Howewer, important results have arisen at the theoretical and algorithmic levels, enabling the characterisation of the regimes for which the solution of nonconvex problems of this class can be reached by convex relaxation [7, 23, 12, 14, 15, 18]. Applications concern scenarios such as low-rank matrix completion, multivariate linear regression, image compression or minimum order linear system realization, see *e.g.*, [23]. Nevertheless, there exists certain instances with a very special structure, which admit closed-form solutions [19, 17]. This occurs typically when the solution can be deduced from the well-known Eckart-Young theorem [6].

Surprisingly, previous works presuppose that problem (1.3) is difficult and does not admit a closed-form solution. Therefore, several sub-optimal approaches are proposed in the literature. In particular, authors in [4, 13] suggest to approach the targeted solution $A_k^\star$ relying on the assumption of linear dependence of recent snapshots on previous ones. This assumption may not be reasonable, especially in the case of non-linear systems. Another approach is to solve the problem, proceeding in two independent steps: first solve problem (1.3) where the low-rank constraint has been removed using SVD as in [26]; then perform a k-th order approximation of the solution using SVD. Finally let us mention that, although it is straightfoward to particularize convex relations techniques to problem (1.3), to the best of our knowledge no algorithm has been dedicated yet to this problem in the literature. It is clear that none of these three approaches will guarantee optimality in general.

The contribution of this paper is threefold. First, we show that the special structure of problem (1.3) enables the characterization of an exact closed-form solution and an easily implementable solver based on SVD. The solution $A_k^\star$ is obtained without any assumption on the structure of the problem, on the contrary to previous works [4, 13]. Second, based on $A_k^\star$, we propose a reduced-order model which enables to approximate the dynamics by means of a low-dimensional recursion. Third, in the context of the analysis of experimental data, we provide an efficient algorithm to compute the low-rank DMD modes and amplitudes, related to the eigendecomposition of $A_k^\star$.

The paper is organized as follows. In Section 2, we provide a brief review of state-of-the-art techniques to solve the low-rank DMD approximation problem and to estimate DMD parameters. Section 3 details our analytical solution and the algorithm solving (1.3). Given this optimal solution, Section 4 then presents the reduced-order model solving (1.2). It also describes the algorithm to compute the parameters of the decomposition (1.4) - (1.5). Finally, a numerical evaluation of the method is presented in Section 5 and concluding remarks are given in a last section.

2. State-Of-The-Art Overview. In what follows, we assume that we have at our disposal N trajectories of T snapshots. We will need in the following some matrix notations. The symbol $\|\cdot\|_F$, $\|\cdot\|_*$, the upper scripts $\cdot^\dagger$ and $\cdot^*$ will respectively refer to the Frobenius norm, the nuclear norm[1], the Moore-Penrose pseudo-inverse and the

[1]The nuclear norm or trace norm of a matrix is the sum of its singular values

transpose operator. I_k will denote the k-dimensional identity matrix. Let consecutive elements of the i-th snapshot trajectory between time t_1 and t_2 be gathered in a matrix $X^i_{t_1:t_2} = (x^i_{t_1}, \cdots, x^i_{t_2})$, and let two large matrices $\mathbf{X}, \mathbf{X'} \in \mathbb{R}^{n\times m}$ with $m = (T-1)N$ be defined as

$$\mathbf{X} = (X^1_{1:T-1}, ..., X^N_{1:T-1}), \quad \mathbf{X'} = (X^1_{2:T}, ..., X^N_{2:T}). \tag{2.1}$$

Without loss of generality, this work will assume that $m \leq n$. We introduce the SVD decomposition of a matrix $M \in \mathbb{R}^{p\times q}$ with $p \geq q$: $M = W_M \Sigma_M V_M^*$ with $W_M \in \mathbb{R}^{p\times q}$, $V_M \in \mathbb{R}^{q\times q}$ and $\Sigma_M \in \mathbb{R}^{q\times q}$ so that $W_M^* W_M = V_M^* V_M = I_q$ and Σ_M is diagonal.

With these notations, problem (1.3) can be rewritten as

$$A_k^\star = \underset{A:\mathrm{rank}(A)\leq k}{\arg\min} \|\mathbf{X'} - A\mathbf{X}\|_F. \tag{2.2}$$

We begin by presenting popular methods of the literature which computes an approximation of the solution of problem (2.2) and related reduced-order models (1.4) - (1.6) solving (1.2).

2.1. Approximation by Low-Rank Projected DMD. As detailed herafter, the original algorithm first proposed for DMD in [24], so-called *projected* DMD in [26], assumes that the snapshots x^i_T for $i = 1, \cdots, N$ can be expressed as a linear combination of the columns of $X^i_{1:T-1}$. This can be written as

$$A\mathbf{X} = \mathbf{X}A^c + R_c. \tag{2.3}$$

In the above equality, the authors of [24, 13] introduce $A^c \in \mathbb{R}^{m\times m}$, the so-called *companion matrix* of A parametrized by m coefficients, and matrix $R_c \in \mathbb{R}^{n\times m}$ whose columns are orthogonal to those of $\mathbf{X}$. Under the assumption used for projected DMD, columns of $A\mathbf{X}$ are in the span of $\mathbf{X}$, so that there exist a matrix A^c such that R_c vanishes. Using the SVD decomposition $\mathbf{X} = W_\mathbf{X} \Sigma_\mathbf{X} V_\mathbf{X}^*$, we notice that in this case we obtain from (2.3) a projected representation of A in the basis spanned by the columns of $W_\mathbf{X}$,

$$W_\mathbf{X}^* A W_\mathbf{X} = \tilde{A}^c, \tag{2.4}$$

where $\tilde{A}^c = \Sigma_\mathbf{X} V_\mathbf{X}^* A^c V_\mathbf{X} \Sigma_\mathbf{X}^{-1} \in \mathbb{R}^{m\times m}$.

Therefore, using this assumption, the low-rank formulation in [13] proposes to approach the solution of (2.2) by determining the m coefficients of matrix A^c which minimize the Frobenius norm of the residual $\mathbf{X'} - A\mathbf{X}$. This yields after some algebraic manipulations to solve the problem

$$\underset{\tilde{A}^c:\mathrm{rank}(\tilde{A}^c\Sigma_\mathbf{X})\leq k}{\arg\min} \|W_\mathbf{X}^* \mathbf{X'} V_\mathbf{X} - \tilde{A}^c \Sigma_\mathbf{X}\|_F. \tag{2.5}$$

The Eckart-Young theorem [6] then provides the optimal solution to this problem based on a rank-k SVD approximation of matrix $B = W_\mathbf{X}^* \mathbf{X'} V_\mathbf{X}$ given by $W_B \Lambda_B V_B^*$ where Λ_B is a diagonal matrix containing only the k-largest singular values of Σ_B and with zero entries otherwhere. Exploiting the low-dimensional representation (2.4), we finally obtain a sub-optimal approximation of the target $A_k^\star$ defined in (2.2)

$$\hat{A}_k = W_\mathbf{X} W_B \Lambda_B V_B^* \Sigma_\mathbf{X}^{-1} W_\mathbf{X}^*. \tag{2.6}$$

A reduced-order model for trajectories is then obtained by using the above the low-rank matrix in recursion (1.2). More precisely, trajectories of (1.2) obey to the k-dimensional recursion (1.6) where we have set $P = W_{\mathbf{X}}$ and $Q = W_B \Lambda_B V_B^* \Sigma_{\mathbf{X}}^{-1} W_{\mathbf{X}}^*$. Moreover, as detailed in [13], an approximation of decomposition (1.4) - (1.5) can also be deduced: approximated low-rank DMD modes are deduced from the eigenvectors of the solution of (2.5) and associated amplitudes are given by solving a convex optimization problem with an iterative gradient-based method.

The SVD involved in the computation of the sub-optimal solution (2.6) bounds the overall complexity of the method to $\mathcal{O}(m^2(m+n))$, *i.e.*, a complexity scaling linearly with the ambient dimension of the high-order model, and cubically with the number of snapshots.

2.2. Approximation by Truncated Non-Projected DMD. As pointed out previously, by removing the low-rank constraint, (2.2) becomes a least-squares problem whose solution is [26]

$$\hat{A}_m = \mathbf{X}'\mathbf{X}^\dagger = \mathbf{X}' V_{\mathbf{X}} \Sigma_{\mathbf{X}}^{-1} W_{\mathbf{X}}^*. \tag{2.7}$$

Let $\hat{A}_{m,k}$ denote a truncation to a rank-k of the SVD decomposition of $\hat{A}_m$. It is important to remark that $\hat{A}_{m,k}$ will generally be a sub-optimal solution of (2.2).

Given $\hat{A}_{m,k}$, low-rank DMD modes can be approximated by its eigenvectors. We note that these eigenvectors are efficiently computed using SVD, see details in [26]. The amplitudes are then derived from the associated eigenvalues according to (1.5). Moreover, trajectories of the reduced-order model (1.2) obey to the k-dimensional recursion (1.6) where we have set $P = W_{\hat{A}_{m,k}}$ and $Q = \Sigma_{\hat{A}_{m,k}} V^*_{\hat{A}_{m,k}}$.

As for the SVD-based approach proposed in Section 2.1, the computation of the sub-optimal solution (2.7) implies an overall complexity scaling in $\mathcal{O}(m^2(m+n))$.

2.3. Approximation by Convex Relaxation. Particularised to problem (2.2), the theoritical results of [15, 12], which are related to the recovery of low-rank matrices in a noisy setting, provide a characterisation of the conditions under which the optimal solution $A_k^\star$ is reached by the following quadratic program

$$\tilde{A}_k^\star = \underset{A \in \mathbb{R}^{n \times n}}{\arg\min} \|\mathbf{X}' - A\mathbf{X}\|_F + \alpha \|A\|_*, \tag{2.8}$$

In the previous optimisation problem, $\alpha \in \mathbb{R}_+$ represents an appropriate parameter determining the rank of $\tilde{A}_k^\star$. The conditions guaranteeing $\tilde{A}_k^\star = A_k^\star$ are expressed in these theoretical works in terms of a so-called *restricted isometry property* that must satisfy the linear operator which maps $A \in \mathbb{R}^{n \times n}$ to $A\mathbf{X} \in \mathbb{R}^{n \times m}$. Program (2.8) is a convex optimization problem which can be solved by standard convex optimization techniques [2], or using dedicated algorithms with increased efficiency as proposed in [12] and [18].

Given $\tilde{A}_k^\star$, we can design a reduced-order model (1.2) taking the form of the k-dimensional recursion (1.6) where we have set $P = W_{\tilde{A}_k^\star}$ and $Q = \Sigma_{\tilde{A}_k^\star} V^*_{\tilde{A}_k^\star}$. Moreover, we can approximate low-rank DMD modes by the eigenvectors of $\tilde{A}_k^\star$ and deduce amplitudes from the associated eigenvalues according to (1.5).

In contrast to the previous approaches, the dedicated algorithms computing $\tilde{A}_k^\star$ present the advantage to involve a low complexity scaling in $\mathcal{O}((m+n)k)$, *i.e.*, linear with respect to the ambient dimension n of the high-order model, but also with

respect to the number of snapshots m. We remark that the construction of reduced-order models (1.4) - (1.6) implies a slight increase of the overall complexity, which scales in $\mathcal{O}((mk+n)k)$.

3. The Proposed Approach. The existence of a closed-form solution to problem (2.2) remains to our knowledge overlooked in the literature, and no exact algorithms have yet been proposed. The following section intends to fill this gap.

3.1. Closed-form Solution to (2.2). Inspired by the framework proposed by *Hasselmann* in [9], we introduce the factorization $A = PQ^*$ in (2.2), with parameters $(P,Q) \in \mathbb{R}^{n\times k} \times \mathbb{R}^{n\times k}$ belonging to the admissible set

$$\Omega = \{(P,Q) \in \mathbb{R}^{n\times k} \times \mathbb{R}^{n\times k} | p_i^* p_i = 1 \quad \text{for} \quad 1 \leq i \leq k\},$$

where the p_i's denote the columns of P. With this parametrization, problem (2.2) can be rewritten as

$$(\hat{P},\hat{Q}) = \underset{(P,Q)\in\Omega}{\arg\min} \|\mathbf{X}' - PQ^*\mathbf{X}\|_F. \tag{3.1}$$

The following theorem provides the closed-form solution to this problem. We detail the proof in the appendix. Consequently, given $(\hat{P},\hat{Q})$, the solution of problem (2.2) writes $A_k^\star = \hat{P}\hat{Q}^*$.

THEOREM 3.1. *A solution of* (3.1) *is*

- $\hat{P} = (\hat{p}_1 \cdots \hat{p}_k)$*, whose columns are real orthonormal eigenvectors associated to the* k *largest eigenvalues of the symetric matrix* $\mathbf{X}'\mathbf{X}^*(\mathbf{X}\mathbf{X}^*)^\dagger\mathbf{X}\mathbf{X}'^*$,
- $\hat{Q} = (\hat{q}_1 \cdots \hat{q}_k)$*, with* $\hat{q}_j = (\mathbf{X}\mathbf{X}^*)^\dagger\mathbf{X}\mathbf{X}'^*\hat{p}_j$*, for* $j = 1, ..., k$.

This solution is unique up to a permutation of the columns of $\hat{P}$ *and* $\hat{Q}$.

3.2. Efficient Solver. The matrix $\mathbf{X}'\mathbf{X}^*(\mathbf{X}\mathbf{X}^*)^\dagger\mathbf{X}\mathbf{X}'^*$ is of size $n \times n$. Since n is typically very large, this prohibits the direct computation of an eigenvalue decomposition. Moreover, a direct calculation of the pseudo-inverse of the $n \times n$ matrix $\mathbf{X}\mathbf{X}^*$ is infeasible. The following well-known remark is useful to overcome these difficulties.

REMARK 1. *The eigenvectors associated to the (at most)* $\ell \leq n$ *non-zero eigenvalues of some matrix* $ZZ^* \in \mathbb{R}^{n\times n}$ *with* $Z \in \mathbb{R}^{n\times \ell}$ *can be obtained from the eigenvectors* $V_Z = (v_1, ..., v_\ell) \in \mathbb{R}^{\ell\times\ell}$ *and eigenvalues* $\sigma = (\sigma_1, ..., \sigma_\ell)$ *of the smaller matrix* $Z^*Z \in \mathbb{R}^{\ell\times\ell}$*. Indeed, the SVD of a matrix* Z *of rank at most* ℓ *is*

$$Z = W_Z \Sigma_Z V_Z^*,$$

with $\Sigma_Z = diag(\sigma^{\frac{1}{2}})$ *and where the columns of matrix* $W_Z \in \mathbb{R}^{n\times\ell}$ *are the eigenvectors of* ZZ^**. Since* V_Z *is unitary, we obtain that the sought vectors are the first* k *columns of* W_Z*, i.e., of* $ZV_Z\, diag(\sigma^{-\frac{1}{2}})$.

In the light of this remark, it is straightforward to design Algorithm 1, which will compute efficiently the solution of (3.1) based on two SVDs. We note that the complexity of this algorithm scaling in $\mathcal{O}(m^2(m+n))$ is identical to state-of-the-art approaches based on SVDs.

Algorithm 1 Solver for (3.1)

inputs: N-sample $\{X^i_{1:T}\}_{i=1}^N$

1) Form matrix $\mathbf{X}$ and $\mathbf{X'}$ as defined in (2.1).

2) Compute the SVD of $\mathbf{X}$.

3) Compute the columns of $\hat{P}$, *i.e.*, the k first eigenvectors of matrix $\mathbf{X'X}^*(\mathbf{XX}^*)^\dagger\mathbf{XX'}^* = \mathbf{X'}V_\mathbf{X}V_\mathbf{X}^*\mathbf{X'}^*$, by making the identification $Z = \mathbf{X'}V_\mathbf{X}$ in Remark 1.

4) Compute the columns of $\hat{Q}$, where the j-th column for $j = 1, ..., k$ is given by

$$\hat{q}_j = W_\mathbf{X}{\Sigma_\mathbf{X}}^{-1}V_\mathbf{X}^*\mathbf{X'}^*\hat{p}_j.$$

outputs: matrix $A_k^\star = \hat{P}\hat{Q}^*$

Algorithm 2 low-rank DMD modes and amplitudes

inputs: matrices $(\hat{P}, \hat{Q})$

1) Compute the SVD of matrix $\hat{Q} = W_Q\Sigma_Q V_Q^*$.

2) Solve for $i = 1, \cdots, k$ the eigen equation

$$\tilde{A}_k w_i = \lambda_i w_i, \quad ,$$

where $w_i \in \mathbb{C}^m$ and $\lambda_i \in \mathbb{C}$ denote eigenvectors and eigenvalues of

$$\tilde{A}_k = W_Q^*\hat{P}V_Q\Sigma_Q \in \mathbb{R}^{m\times m}.$$

3) The i-th DMD mode corresponding to the eigenvalue λ_i is then given by

$$\phi_i = W_Q w_i.$$

outputs: DMD modes ϕ_i and eigenvalues λ_i for $i = 1, \cdots, k$

4. Reduced-Order Models. Given the solution $A_k^\star = \hat{P}\hat{Q}^*$ of (3.1), we discuss in what follows the construction of reduced-order models to solve (1.2). We first focus on building a k-dimensional recursion based on $(\hat{P}, \hat{Q})$. We then detail the computation of the low-rank DMD parameters, *i.e.*, modes and associated amplitudes. Let us remark that these operations do not increase the overall complexity, since they require a lower complexity than for computing the optimal solution $A_k^\star$ with Algorithm 1.

4.1. Trajectory Approximation by a Low-Dimensional Recursion. Trajectories of (1.2) are fully determined by the k-dimensional recursion (1.6) where $P = \hat{P}$ and $Q = \hat{Q}$. That is to say, we first compute for all $i = 1, \cdots, N$ the trajectory of the projected variable $z_t^i = \hat{P}^*\tilde{x}_t^i$

$$\begin{cases} z_t^i = \hat{Q}^*\hat{P}z_{t-1}^i, \\ z_1^i = \hat{P}^*\tilde{x}_1^i. \end{cases} \tag{4.1}$$

By multiplying both sides by matrix $\hat{P}$, we then obtain for $i = 1, \cdots, N$ the sought low-rank approximations $\tilde{x}_t^i = \hat{P}z_t^i$.

4.2. Trajectory Approximation by Identification of DMD Parameters. Low-rank DMD modes and amplitudes have a closed-form expression, and their computation does not involve any minimization procedure, on the contrary to what is proposed by the author in [13]. Indeed, the i-th DMD mode $\phi_i \in \mathbb{C}^n$ is the eigenvector of $\hat{P}\hat{Q}^*$ associated to the i-th largest eigenvalue $\lambda_i \in \mathbb{C}$. As detailed in Algorithm 2 and proved in Remark 2, the eigendecomposition of $\hat{P}\hat{Q}^*$ can be efficiently performed using SVDs.

REMARK 2. *Each pair (ϕ_i, λ_i) generated by Algorithm 2 is one of the k eigenvector/eigenvalue pair of $\hat{A}_k$. Indeed, by definition we have $\hat{A}_k = \hat{P}V_Q\Sigma_Q W_Q^*$. Furthermore, $\tilde{A}_k = W_Q^*\hat{P}V_Q\Sigma_Q$ and $\phi_i = \frac{1}{\lambda_i}PV_Q\Sigma_Q w_i$. Therefore, we have*

$$\hat{A}_k\phi_i = \frac{1}{\lambda_i}\hat{P}V_Q\Sigma_Q W_Q^*\hat{P}V_Q\Sigma_Q w_i = \hat{P}V_Q\Sigma_Q\frac{1}{\lambda_i}\tilde{A}_k w_i = \hat{P}V_Q\Sigma_Q w_i = \lambda_i\phi_i.$$

Using $\{(\phi_i, \lambda_i)\}_{i=1}^k$ in (1.4) - (1.5), one obtains a low-rank approximation of the j-th snapshot $\tilde{x}_t^j$ in terms of DMD modes and amplitudes.

5. Numerical Evaluation. In what follows, we evaluate the different approaches for low-rank approximations of system (1.1) by DMD. We assess three different methods for computing $\hat{A}_k$:

- method *a*), optimal rank-k approximation given by Algorithm 1,
- method *b*), k-th order SVD approximation of (2.7), *i.e.*, k-th order approximation of the rank-m non-projected DMD solution [26],
- method *c*), rank-k approximation by (2.6), corresponding to the projected DMD approach [13] (or [24] for $k \geq m$).

Convex relaxation approaches have been omitted in the present evaluation because there does not exist in the literature an algorithm coding the recovery of $\hat{A}_k$ yet. Nevertheless, we mention that, because of their attractive complexity scaling linearly in m, it would be interesting to evaluate the performance of these sub-optimal algorithms which are well-suited to tackle the case of a large number of snapshots.

The performance is measured in terms of the error norm $\|\mathbf{X}' - \hat{A}_k\mathbf{X}\|_F$ with respect to the rank k. We begin by evaluating the low-rank approximations using a toy model and then continue by assessing their performances for the reduction of a Rayleigh-Bénard convective system. We finally evaluate Algorithm 2 and in particular the influence of noise on the capability of the method to extract accurate DMD parameters.

5.1. Toy model. We consider a high-dimensional space of $n = 50$ dimensions, a low-dimensional subspace of $r = 30$ dimensions and $m = 40$ snapshots. Let G be a matrix of rank r generated randomly according to $G = \sum_{i=1}^r \xi_i\xi_i^*$, where entries of ξ_i's are n independent samples of the standard normal distribution. Let the initial condition θ be randomly chosen according to the same distribution. The snapshots, gathered in matrices $\mathbf{X}$ and $\mathbf{X}'$, are generated using (1.1) for three configurations of f_t:

- setting *i)*, $f_t(x_{t-1}) = Gx_{t-1}$, s.t. $\exists A^c$ satisfying $G\mathbf{X} = \mathbf{X}A^c$,
- setting *ii*), $f_t(x_{t-1}) = Gx_{t-1}$,
- setting *iii*), $f_t(x_{t-1}) = Gx_{t-1} + G\text{diag}(x_{t-1})\text{diag}(x_{t-1})x_{t-1}$.

Setting i) corresponds to a linear system satisfying the assumption that snapshots are linearly dependent, as made in the projected DMD approaches [24, 13]. Setting ii) and iii), do not make this assumption and simulate respectively linear and non-linear dynamical systems.

Results for the three settings are displayed in Figure 5.1. As a first remark, we notice that the solution provided by Algorithm 1 (method a) yields the best results, in agreement with Theorem 3.1.

Second, in setting i), the experiments confirm that when the linearity assumption is valid, the low-rank projected DMD (method c) achieves the same performance as the optimal solution (method a). Moreover, truncating the rank-m DMD solution (method b) induces as expected an increase of the error norm. This deterioration is however moderate in our experiments.

Then, in settings ii) and iii) we remark that the behavior of the error norms are analogous (up to an order of magnitude). The performances of the projected approach (method c) differs notably from the optimal solution. A significant deterioration is visible for $k > 10$. This is the consequence of the non-validity of the linear dependence assumed in method c. Nevertheless, we notice that method c accomplishes a slight gain in performance compared to method b up to a moderate rank ($k < 5$). Besides, we also notice that the error norm of method b in the case $k < 30$ is not optimal.

Finally, as expected, all methods succeed in properly characterizing the low-dimensional subspace as soon as $k \geq r$.

5.2. Geophysical Model. We next evaluate the low-rank approximation of a Rayleigh-Bénard convective system [3]. This geophysical model is at the origin of the famous Lorenz reduced system (obtained by Galerkin projection), whose solution, when plotted, resemble a butterfly [16]. An incompressible fluid is contained in a bi-dimensional cell and is subject to periodic boundary conditions. The states of interest are the trajectories of the temperature and of the velocity in the cell. Let differential operators $\nabla = (\partial_{s_1}, \partial_{s_2})^*$ and $\Delta = \partial_{s_1}^2 + \partial_{s_2}^2$ denote the gradient and the Laplacian with respect to the two spatial dimensions (s_1, s_2). Let operator Δ^{-1} be the inverse of Δ. Convection is driven by the two following coupled partial differential equations. At any point of the unit cell $\mathbf{s} = (s_1, s_2) \in [0, 1]^2$ and for any time $t \in \mathbb{R}_+$, we have

$$\begin{cases} \partial_t b(\mathbf{s}, t) + \mathbf{v}(\mathbf{s}, t) \cdot \nabla b(\mathbf{s}, t) - \sigma \Delta b(\mathbf{s}, t) - \sigma \nu \partial_{s_1} \tau(\mathbf{s}, t) = 0, \\ \partial_t \tau(\mathbf{s}, t) + \mathbf{v}(\mathbf{s}, t) \cdot \nabla \tau(\mathbf{s}, t) - \Delta \tau(\mathbf{s}, t) - \partial_{s_1} \Delta^{-1} b(\mathbf{s}, t) = 0, \end{cases} \tag{5.1}$$

where $\tau(\mathbf{s}, t) \in \mathbb{R}$ and $\mathbf{v}(\mathbf{s}, t) \in \mathbb{R}^2$ are the temperature and the velocity and where the buoyancy $b(\mathbf{s}, t) \in \mathbb{R}$ satisfies

$$\mathbf{v}(\mathbf{s}, t) = \nabla^\perp \Delta^{-1} b(\mathbf{s}, t).$$

The Rayleigh number $\sigma \in \mathbb{R}_+$ controls the balance between thermal diffusion and the tendency for a packet of fluid to rise due to the buoyancy force. The Prandtl number $\nu \in \mathbb{R}_+$ measures the relative importance of viscosity compared to thermal diffusion. At initial time $t = 0$, the fluid in the cell is still and subject to a difference of temperature between the bottom and the top.

In our experiments, we assume the initial condition is solution of the Lorenz

model [16]

$$\begin{aligned} b(\mathbf{s},0) =& \kappa_b \sin(a_b s_1)\sin(\pi s_2), \\ \tau(\mathbf{s},0) =& \kappa_{\tau_1}\cos(a_\tau s_1)\sin(\pi s_2) - \kappa_{\tau_1}\sin(2\pi s_2). \end{aligned} \tag{5.2}$$

It is easy to verify that for this parametrization and in the particular case where $\nu = 0$ and $\kappa_b = \sigma^{-1}(\pi a)^{-2}$, the non-linear system (5.1) simplifies into a linear temperature evolution driven by a (non-stationary) buoyancy force associated to a Taylor vortex [25]

$$\begin{cases} b(\mathbf{s},t) = \sigma^{-1}(\pi a_b)^{-2}\exp^{-\sigma\pi^2 a_b^2 t}\sin(a_b s_1)\sin(\pi s_2), \\ \partial_t \tau(\mathbf{s},t) + \mathbf{v}(\mathbf{s},t)\cdot\nabla\tau(\mathbf{s},t) - \Delta\tau(\mathbf{s},t) - \partial_{s_1}\Delta^{-1} b(\mathbf{s},t) = 0. \end{cases} \tag{5.3}$$

Using finite difference approximations, we obtain discrete systems of the form of (1.1) with $x_t = \begin{pmatrix} b_t \\ \tau_t \end{pmatrix} \in \mathbb{R}^n$, and $n = 1024$, where b_t's and τ_t's are spatial discretisations of buoyancy and temperature fields at time t. We assume that we have at our disposal three datasets of snapshots of the discretized system trajectories, revealing either linear or non-linear settings. More precisely, we choose $m = 50$ and the three following datasets:

- setting iv), $N = 50$ short trajectories ($T = 2$) of the linear system (5.3) obtained by fixing the initial condition (5.2) with random parameters $(a_\tau, \kappa_{\tau_1}, \kappa_{\tau_2})$ and setting $a_b = 1$,
- setting v), $N = 5$ long trajectories ($T = 11$) of the linear system (5.3) obtained by fixing the initial condition (5.2) with random parameters $(a_\tau, \kappa_{\tau_1}, \kappa_{\tau_2})$ and setting $a_b = 1$,
- setting vi), $N = 5$ long trajectories ($T = 11$) of the non-linear system (5.1) obtained by fixing the initial condition (5.2) with random parameters $(a_\tau, \kappa_b, \kappa_{\tau_1}, \kappa_{\tau_2})$ and setting $a_b = a_\tau$.

The parameters are randomly sampled so that each set of initial conditions correspond to N realizations of the uniform distribution over a compact of dimensionality $r = 10$. Results for these three settings are displayed in Figure 5.2.

We first comment on results obtained in setting iv). We remark that, as expected for the situation $T = 2$, the error obtained for the optimal solution (method a) vanishes for $k \geq r$, *i.e.*, a dimensionality greater than the initial condition dimensionality. The sub-optimal solution provided by method b) induces an important error which vanishes only for $k = m$, *i.e.*, for a dimensionality equal to the number of snapshots. Concerning method c), it produces a fairly good solution up to $k \leq 8$, but the solution is clearly sub-optimal for greater dimensions and is associated to an error saturating to a non-negligible value.

In setting v), we have longer sequences ($T > 2$) so that the dimension embedding the initial condition does not necessarily match the dimension embedding the snapshots. However, we remark that the optimal solution provided by method a) induces an error nearly vanishing for $k \geq 10$. This attests of the fact that, for this linear model, trajectories are concentrate near the subspace spanned by the initial condition. This explains the quasi-optimal performances of method c) which relies on a strong assumption of linear dependance of snapshots. Method b) is again clearly sub-optimal and behaves analogously to setting iv).

In the more realistic setting *vi*), we see that the optimal performances achieved by method *a*) are far from being reached by the method *b*) and *c*). As in the linear settings, we observe that the optimal error nearly vanishes for $k \geq 10$. However, we clearly notice that the assumption on which rely method *c*) is for this non-linear model invalide, which induces an error saturating to a non-negligible value. We observe again in this case the poor performance of method *b*).

5.3. Identification of DMD Parameters. In the following, we intend to evaluate the capabilities of the different methods to extract low-rank DMD modes and amplitude in the presence of noise. To this aim, we build a dataset of $N = 5$ long trajectories with $T = 11$ (so that we get $m = 50$ snapshots) satisfying (1.4) - (1.5) with $k = 3$ modes and amplitude $\{(\phi_i, \lambda_i)\}_{i=1}^3$. The latter are extracted using Algorithm 2 from the geophysical dataset described in setting *vi*). We consider the two following configurations:

- setting *vii*), the original version of this dataset,
- setting *viii*), a noisy version, where we have corrupted the snapshots with a zero-mean Gaussian noise so that the peak-to-signal-ratio is 40.

Results are displayed in Figure 5.3 and 5.4.

As expected we recover a vanishing optimal error for method *a*) in the case $k \geq r$. We remark that the error is very similar in the noiseless and in the noisy settings. This attests of the robustness of method *a*) to noise. Unsurprisingly for these two settings, method *c*) reproduces almost exactly the optimal behaviour, although one can notice in the noisy setting and for $k \geq r$ a slight bias with the optimal error. In contrast method *b*) produces clearly sub-optimal solutions in the noiseless setting. More importantly, the performance of this method becomes dramatic in the presence of noise. The deterioration is clearly visible in DMD mode estimates displayed in Figure 5.4. The spatial structure of the DMD mode estimated by method *b*) is completely rubbed out in the noisy setting while it is fairly preserved by method *a*) and *c*). This illustrates the usefulness of solving the low-rank DMD problem instead of truncating the full-rank DMD solution.

6. Conclusion. Following recent attempts to characterize low-rank DMD approximations, this paper provides a closed-form solution to this nonconvex optimization problem. To the best of our knowledge, state-of-the-art methods are all sub-optimal. The paper further proposes effective algorithms based on SVD to solve this problem and run the reduced-order model. Our numerical experiments attest that the proposed algorithm is more accurate than state-of-the-art methods. In particular, we illustrate the fact that simply truncating the full-rank DMD solution, or exploiting a strong assumption of linear dependence of snapshots is insufficient.

Appendix A. Theorem's proof.

We provide hereafter a closed-form solution of (3.1) inspired by the partial demonstration in [9]. Before exposing the proof in details, let us provide a sketch of it. We will first focus on the solutions of (3.1) over a relaxed admissible set: we will characterize solutions of the relaxed problem

$$(\hat{P}', \hat{Q}') = \underset{(P,Q)\in\Omega'}{\arg\min} \|\mathbf{X}' - PQ^*\mathbf{X}\|_F, \tag{A.1}$$

where

$$\Omega' = \{(P, Q) \in \mathbb{R}^{n\times k} \times \mathbb{R}^{n\times k}\},$$

is the original admissible set Ω without the normalisation constraints on the column of P. In order to characterise these solutions, we will begin by showing by induction that the first-order optimality condition consists on two eigenvalue equations on the columns of $P = (p_1, \cdots, p_{j_k})$ and $Q = (q_{j_1}, \cdots, q_{j_k})$. More precisely for $\ell = 1, \cdots, k$, necessary optimality conditions will be

$$\begin{cases} \mathbf{X}'\mathbf{X}^* q_{j_\ell} = \lambda'_{j_\ell} p_{j_\ell}, \\ (\mathbf{X}\mathbf{X}^*)^\dagger \mathbf{X}\mathbf{X}'^* p_{j_\ell} = \lambda''_{j_\ell} q_{j_\ell}, \end{cases} \tag{A.2}$$

for some appropriate scalar λ'_{j_ℓ}, $\lambda''_{j_\ell} \in \mathbb{R}$. We will continue by showing that solutions of (A.1) take the form of matrices, whose columns are the k-first eigenvectors solution of this coupled eigenvalue equation. Adding the normalisation constraints on the column of P to Ω', we finally characterise the unique solution of (3.1) claimed by the theorem: the j-th columns of matrices $(\hat{P}, \hat{Q})$ satisfy

$$\begin{cases} \mathbf{X}'\mathbf{X}^*(\mathbf{X}\mathbf{X}^*)^\dagger \mathbf{X}\mathbf{X}'^* p_j = \lambda_j p_j, \\ q_j = (\mathbf{X}\mathbf{X}^*)^\dagger \mathbf{X}\mathbf{X}'^* p_j, \end{cases} \tag{A.3}$$

for some $\lambda_j \in \mathbb{R}$.

In order to alleviate notations in what follows, we will note the arithmetical average of a function φ of N trajectories between t_1 and t_2 as

$$\tilde{\mathbb{E}}[\varphi(X_{t_1:t_2})] = \sum_{i=1}^{N} \varphi(X^i_{t_1:t_2}),$$

where we have denoted the set of N trajectories by $X_{t_1:t_2} = (x_{t_1}, \cdots, x_{t_2})$ with $x_{t_j} = \{x^i_{t_j}\}_{i=1}^N$.

Let us now expose the detailed proof. As mention above, we claim that a global minimizer of (A.1) satisfies a coupled eigenvalue equation of the form of (A.2). To prove this, we use an induction argument. We first show the base case, *i.e.*, that a global minimizer of (A.1) for $k = 1$ denoted $(\hat{p}'_{j_1}, \hat{q}'_{j_1})$, must satisfy an eigenvalue equation. From the first-order optimality condition arising from problem (A.1), we obtain that $(\hat{p}'_{j_1}, \hat{q}'_{j_1})$ should solve

$$\begin{cases} \displaystyle\sum_{t=1}^{T-1} \tilde{\mathbb{E}}[(x_t^* q_{j_1})(x_{t+1} - p_{j_1} q^*_{j_1} x_t)] = 0, \\ \displaystyle\sum_{t=1}^{T-1} \tilde{\mathbb{E}}[x_t(p^*_{j_1}(x_{t+1} - p_{j_1} q^*_{j_1} x_t))] = 0. \end{cases}$$

The latter equalities may be rewritten as

$$\begin{cases} \mathbf{X}'\mathbf{X}^* q_{j_1} = \tilde{\mathbb{E}}[\displaystyle\sum_{t=1}^{T-1} (q^*_{j_1} x_t)^2] p_{j_1}, \\ \mathbf{X}\mathbf{X}'^* p_{j_1} = \mathbf{X}\mathbf{X}^*(p^*_{j_1} p_{j_1}) q_{j_1}, \end{cases}$$

and by multiplying the second equation by $(\mathbf{X}\mathbf{X}^*)^\dagger$ we obtain two coupled eigenvalue equations

$$\begin{cases} Cq_{j_1} = \lambda'_{j_1} p_{j_1}, \\ \bar{C}p_{j_1} = \lambda''_{j_1} q_{j_1}, \end{cases} \tag{A.4}$$

where

$$C = \mathbf{X}'\mathbf{X}^*, \tag{A.5}$$

$$\bar{C} = (\mathbf{X}\mathbf{X}^*)^\dagger \mathbf{X}\mathbf{X}'^*, \tag{A.6}$$

$$\lambda'_{j_1} = \tilde{\mathbb{E}}[\sum_{t=1}^{T-1} (q_{j_1}^* X_t)^2], \tag{A.7}$$

$$\lambda''_{j_1} = p_{j_1}^* p_{j_1}. \tag{A.8}$$

Separation of p_{j_1} and q_{j_1} then yields the pair of eigenvalue equations

$$\begin{cases} C\bar{C}p_{j_1} = \lambda_{j_1} p_{j_1}, \\ \bar{C}Cq_{j_1} = \lambda_{j_1} q_{j_1}, \end{cases} \tag{A.9}$$

with the same eigenvalues

$$\lambda_{j_1} = \lambda'_{j_1} \lambda''_{j_1}, \tag{A.10}$$

for p_{j_1} and q_{j_1}. We remark in (A.9) that $C\bar{C}$ is a symmetrical, semi-positive definite matrix and that $\bar{C}C$ consists of quadratic products of symmetrical, semi-positive definite matrices. It follows that these matrices are diagonalisable with real and positive eigenvalues, see *e.g.*, [11, Corrollary 7.6.2]. These eigenvalues are associated to real eigenvectors. Note that eigenvectors of $C\bar{C}$ are orthogonal, while this is not necessarily the case for the eigenvectors of $\bar{C}C$.

From the base case condition (A.4) - (A.9) satisfied by a solution $(\hat{p}'_1, \hat{q}'_1)$ of (A.1) for $k = 1$, we now show by induction that, for an arbitrary k, the columns $\{(\hat{p}'_{j_i}, \hat{q}'_{j_i}); 1 \leq j_i \leq k\}$ of a minimizer $(\hat{P}', \hat{Q}')$ of problem (A.1) should necessarily be solution of the same eigenvector equations, *i.e.*, satisfy the coupled

$$\begin{cases} Cq_{j_i} = \lambda'_{j_i} p_{j_i}, \\ \bar{C}p_{j_i} = \lambda''_{j_i} q_{j_i}, \end{cases} \tag{A.11}$$

and decoupled system

$$\begin{cases} C\bar{C}p_{j_i} = \lambda_{j_i} p_{j_i}, \\ \bar{C}Cq_{j_i} = \lambda_{j_i} q_{j_i}. \end{cases} \tag{A.12}$$

Note that eigenvectors solution of (A.12) are solution of (A.11) for eigenvalues λ'_j and λ''_j satisfying

$$\lambda_{j_i} = \lambda'_{j_i} \lambda''_{j_i}.$$

The induction assumption is that the columns of a local minimizer of problem (A.1) with $k = \ell$ denoted $\hat{P}'_{j_1:j_\ell}$ and $\hat{Q}'_{j_1:j_\ell}$ satisfy (A.11) - (A.12). We saw that this stands

for the base case, *i.e.*, for $k = 1$, according to (A.9). We then need to show that a local minimizer $(\hat{p}_{j_{\ell+1}}, \hat{q}_{j_{\ell+1}})$ of the problem with $k = \ell + 1$ where the ℓ first columns of $(\hat{P}', \hat{Q}')$, *i.e.*, $(\hat{P}'_{j_1:j_\ell}, \hat{Q}'_{j_1:j_\ell})$ satisfy the induction assumption, satisfies also (A.12). Expanding the cost to be minimized with respect to $(p_{j_{\ell+1}}, q_{j_{\ell+1}})$, we have

$$\tilde{\mathbb{E}}[\|X_{2:T} - \hat{P}_{j_1:j_\ell}\hat{Q}^*_{j_1:j_\ell}X_{1:T-1} - p_{j_{\ell+1}}q^*_{j_{\ell+1}}X_{1:T-1}\|_F^2] = \tilde{\mathbb{E}}[\|X_{2:T} - \hat{P}_{j_1:j_\ell}\hat{Q}^*_{j_1:j_\ell}X_{1:T-1}\|_F^2]$$
$$\sum_{t=2}^{T} p^*_{j_{\ell+1}}p_{j_{\ell+1}}\tilde{\mathbb{E}}[(q^*_{j_{\ell+1}}x_{t-1})^2] - 2p^*_{j_{\ell+1}}\tilde{\mathbb{E}}[(x_t - \hat{P}_{j_1:j_\ell}\hat{Q}^*_{j_1:j_\ell}x_{t-1})x^*_{t-1}]q_{j_{\ell+1}}.$$

From the optimality condition, we obtain after some simple calculation that $(\hat{p}_{j_{\ell+1}}, \hat{q}_{j_{\ell+1}})$ should satisfy

$$\begin{cases} \lambda'_{j_{\ell+1}}p_{j_{\ell+1}} - \sum_{t=2}^{T}(\tilde{\mathbb{E}}[x_t x^*_{t-1}] - \hat{P}_{j_1:j_\ell}\hat{Q}^*_{j_1:j_\ell}\tilde{\mathbb{E}}[x_{t-1}x^*_{t-1}])q_{j_{\ell+1}} = 0, \\ \sum_{t=2}^{T}\lambda''_{j_{\ell+1}}\tilde{\mathbb{E}}[x_{t-1}x^*_{t-1}]q_{j_{\ell+1}} - (\tilde{\mathbb{E}}[x_{t-1}x^*_t] - \tilde{\mathbb{E}}[x_{t-1}x^*_{t-1}]\hat{Q}_{j_1:j_\ell}\hat{P}^*_{j_1:j_\ell})p_{j_{\ell+1}} = 0, \end{cases}$$

where we have used analogous notations to the one used in (A.7) - (A.8). By multiplying the second equation by $(\mathbf{X}\mathbf{X}^*)^\dagger$ we obtain two coupled eigenvalue equations

$$\begin{cases} C'q_{j_{\ell+1}} = \lambda'_{j_{\ell+1}}p_{j_{\ell+1}}, \\ \bar{C}'p_{j_{\ell+1}} = \lambda''_{j_{\ell+1}}q_{j_{\ell+1}}, \end{cases} \tag{A.13}$$

where we have introduced the matrices

$$C' = \mathbf{X}'\mathbf{X}^* - \hat{P}_{j_1:j_\ell}\hat{Q}^*_{j_1:j_\ell}\mathbf{X}\mathbf{X}^*, \tag{A.14}$$
$$\bar{C}' = (\mathbf{X}\mathbf{X}^*)^\dagger\mathbf{X}\mathbf{X}'^* - \hat{Q}_{j_1:j_\ell}\hat{P}^*_{j_1:j_\ell}, \tag{A.15}$$

Separation of $p_{j_{\ell+1}}$ and $q_{j_{\ell+1}}$ then yields the pair of eigenvalue equations

$$\begin{cases} C'\bar{C}'p_{j_{\ell+1}} = \lambda_{j_{\ell+1}}p_{j_{\ell+1}}, \\ \bar{C}'C'q_{j_{\ell+1}} = \lambda_{j_{\ell+1}}q_{j_{\ell+1}}, \end{cases} \tag{A.16}$$

where we have used a notation analogous to (A.10). By simple linear algebraic manipulation and using (A.11), we obtain

$$\begin{cases} C'\bar{C}' = (\mathbf{I}_n - \hat{P}_{j_1:j_\ell}\,\mathrm{diag}(1/\lambda''_{j_1:\ell})\hat{P}^*_{j_1:j_\ell})C\bar{C}(\mathbf{I}_n - \hat{P}_{j_1:j_\ell}\,\mathrm{diag}(1/\lambda''_{j_1:\ell})\hat{P}^*_{j_1:j_\ell}), \\ \bar{C}'C' = \bar{C}C - \hat{Q}_{j_1:j_\ell}\,\mathrm{diag}(1/\lambda_{j_1:\ell})\hat{Q}^*_{j_1:j_\ell}C^*C. \end{cases} \tag{A.17}$$

The first equations of (A.17) shows that the column of $C'\bar{C}'$ are the projection of the columns of $C\bar{C}$ onto the space spanned by the ℓ first eigenvectors, *i.e.*, the columns of matrix $\hat{P}'_{j_1:j_\ell}$. Therefore, the eigenvectors of $C'\bar{C}'$ are the eigenvectors of $C\bar{C}$ associated to the $n - \ell$ lowest eigenvalues. This includes in particular $\hat{p}'_{j_{\ell+1}}$. Besides, by multiplying the second equation of (A.17) by any eigenvectors $\hat{q}'_{j_i}$ of $\bar{C}C$ with $1 \le i \le n$, using (A.11) and (A.12) we obtain

$$\bar{C}'C'\hat{q}'_{j_i} = \begin{cases} (1 - 1/\lambda''_{j_i})\lambda_{j_i}\hat{q}'_{j_i}, & \text{for} \quad 1 \le i \le \ell \\ \lambda_{j_i}\hat{q}'_{j_i}, & \text{for} \quad \ell < i \le n \end{cases}$$

which shows that $\bar{C}'C'$ and $\bar{C}C$ possess the same eigenvectors[2]. Therefore, $(\hat{p}'_{j_{\ell+1}}, \hat{q}'_{j_{\ell+1}})$ are solution of (A.12), which concludes the proof by induction.

We continue by showing that a global minimum, *i.e.*, a closed-form solution of (A.1), is reached for matrices $\hat{P} = (\hat{p}_1, ..., \hat{p}_k)$ and $\hat{Q} = (\hat{q}_1, ..., \hat{q}_k)$, whose columns are the eigenvectors associated to the k largest eigenvalues $\{\lambda_j\}_{j=1}^k$ with $\lambda_j \geq \lambda_{j+1}$. Indeed, by simple calculation and using (A.8) we obtain

$$\tilde{\mathbb{E}}[\|X_{2:T} - (\hat{p}_{j_1}, ..., \hat{p}_{j_k})(\hat{q}_{j_1}, ..., \hat{q}_{j_k})^* X_{1:T-1}\|_F^2] = \sum_{j=j_1}^{j_k} (\lambda''_j \tilde{\mathbb{E}}[\sum_{t=1}^{T-1} (\hat{q}_j^* x_t)^2])$$
$$+ \tilde{\mathbb{E}}[\|X_{2:T}\|_F^2] - 2\,\mathrm{trace}\left((\hat{p}_{j_1}, ..., \hat{p}_{j_k})^* \tilde{\mathbb{E}}[X_{2:T} X_{1:T-1}^*](\hat{q}_{j_1}, ..., \hat{q}_{j_k})\right),$$

where each element of the set of indices $\{j_1, ..., j_k\}$ is a positive integer smaller or equal to n. Using (A.5), (A.7), (A.10) and (A.11) , we obtain

$$\begin{aligned}
&\tilde{\mathbb{E}}[\|X_{2:T} - (\hat{p}_{j_1}, ..., \hat{p}_{j_k})(\hat{q}_{j_1}, ..., \hat{q}_{j_k})^* X_{1:T-1}\|_F^2] \\
&= \sum_{j=j_1}^{j_k} \lambda_j + \tilde{\mathbb{E}}[\|X_{2:T}\|_F^2] - 2 \sum_{j=j_1}^{j_k} \mathrm{trace}[\,(\hat{p}_{j_1}, ..., \hat{p}_{j_k})^* (\lambda'_{j_1} \hat{p}_{j_1}, \cdots, \lambda'_{j_k} \hat{p}_{j_k})], \\
&= \sum_{j=j_1}^{j_k} \lambda_j + \tilde{\mathbb{E}}[\|X_{2:T}\|_F^2] - 2 \sum_{j=j_1}^{j_k} \lambda_j, \\
&= \tilde{\mathbb{E}}[\|X_{2:T}\|_F^2] - \sum_{j=j_1}^{j_k} \lambda_j. \qquad \text{(A.18)}
\end{aligned}$$

As a result, we have the problem equivalence

$$\arg\min_{(j_1,...,j_k)} \tilde{\mathbb{E}}[\|X_{2:T} - (\hat{p}_{j_1}, ..., \hat{p}_{j_k})(\hat{q}_{j_1}, ..., \hat{q}_{j_k})^* X_{1:T-1}\|_F^2] = \arg\max_{(j_1,...,j_k)} \sum_{j=j_1}^{j_k} \lambda_j,$$

whose solution is the set of indices $\{j_\ell\}_{\ell=1}^k$ where j_ℓ's are strictly positive integers smaller or equal to k. Clearly, a global minimizer satisfies $j_\ell \neq j_r$ for $\ell \neq r$ (otherwise matrix $\hat{P}\hat{Q}^*$ would be of rank lower than k and the minimum of (A.18) would not be reached). Note that we are searching an non-order set of indices, so that it is sufficient to choose the minimizing set $(j_1, ..., j_k) = (1, ..., k)$.

We conclude the proof by imposing the normalization constraints $\lambda''_\ell = 1$ for $\ell = 1, \cdots, k$, which reduces the admissible set from Ω' to Ω. We obtain the necessary condition (A.3). It is clear that, up to some column permutation, the minimizer satisfying these coupled eigenvalue equations is unique and specifies a unique solution to problem (3.1).

[2]Note that if we are interested in the case $\lambda''_{j_i} = 1$, the ℓ eigenvectors $\{\hat{q}_{j_i}; 1 \leq i \leq \ell\}$ already extracted from matrix $\bar{C}C$ are associated to zero eigenvalues in matrix $\bar{C}'C'$.

REFERENCES

[1] Antoulas, A.C.: An overview of approximation methods for large-scale dynamical systems. Annual Reviews in Control **29**(2), 181–190 (2005)

[2] Bertsekas, D.: Nonlinear Programming. Athena Scientific (1995). URL `https://books.google.ie/books?id=QeweAQAAIAAJ`

[3] Chandrasekhar, S.: Hydrodynamic and hydromagnetic stability. Courier Corporation (2013)

[4] Chen, K.K., Tu, J.H., Rowley, C.W.: Variants of dynamic mode decomposition: boundary condition, koopman, and fourier analyses. Journal of nonlinear science **22**(6), 887–915 (2012)

[5] Cohen, A., Devore, R.: Approximation of high-dimensional parametric PDEs. ArXiv e-prints (2015)

[6] Eckart, C., Young, G.: The approximation of one matrix by another of lower rank. Psychometrika **1**(3), 211–218 (1936)

[7] Fazel, M.: Matrix rank minimization with applications, stanford university. Ph.D. thesis (2002)

[8] Fink, J.P., Rheinboldt, W.C.: On the error behavior of the reduced basis technique for nonlinear finite element approximations. ZAMM - Journal of Applied Mathematics and Mechanics **63**(1), 21–28 (1983)

[9] Hasselmann, K.: PIPs and POPs: The reduction of complex dynamical systems using principal interaction and oscillation patterns. Journal of Geophysical Research: Atmospheres **93**(D9), 11,015–11,021 (1988)

[10] Holmes, P., Lumley, J.L., Berkooz, G.: Turbulence, Coherent Structures, Dynamical Systems and Symmetry. Cambridge University Press (1996). Cambridge Books Online

[11] Horn, R.A., Johnson, C.R.: Matrix analysis. Cambridge university press (2012)

[12] Jain, P., Meka, R., Dhillon, I.S.: Guaranteed rank minimization via singular value projection. In: Advances in Neural Information Processing Systems, pp. 937–945 (2010)

[13] Jovanovic, M., Schmid, P., Nichols, J.: Low-rank and sparse dynamic mode decomposition. Center for Turbulence Research Annual Research Briefs pp. 139–152 (2012)

[14] Lee, K., Bresler, Y.: Guaranteed minimum rank approximation from linear observations by nuclear norm minimization with an ellipsoidal constraint. arXiv preprint arXiv:0903.4742 (2009)

[15] Lee, K., Bresler, Y.: Admira: Atomic decomposition for minimum rank approximation. IEEE Transactions on Information Theory **56**(9), 4402–4416 (2010)

[16] Lorenz, E.N.: Deterministic Nonperiodic Flow. Journal of Atmospheric Sciences **20**, 130–148 (1963)

[17] Mesbahi, M., Papavassilopoulos, G.P.: On the rank minimization problem over a positive semidefinite linear matrix inequality. IEEE Transactions on Automatic Control **42**(2), 239–243 (1997)

[18] Mishra, B., Meyer, G., Bach, F., Sepulchre, R.: Low-rank optimization with trace norm penalty. SIAM Journal on Optimization **23**(4), 2124–2149 (2013)

[19] Parrilo, P.A., Khatri, S.: On cone-invariant linear matrix inequalities. IEEE Transactions on Automatic Control **45**(8), 1558–1563 (2000)

[20] Peherstorfer, B., Willcox, K.: Data-driven operator inference for nonintrusive projection-based model reduction. Computer Methods in Applied Mechanics and Engineering **306**, 196–215 (2016)

[21] Penland, C., Magorian, T.: Prediction of nino 3 sea surface temperatures using linear inverse modeling. Journal of Climate **6**(6), 1067–1076 (1993)

[22] Quarteroni, A., Rozza, G., Manzoni, A.: Certified reduced basis approximation for parametrized partial differential equations and applications. Journal of Mathematics in Industry **1**(1), 1–49 (2011)

[23] Recht, B., Fazel, M., Parrilo, P.A.: Guaranteed minimum-rank solutions of linear matrix equations via nuclear norm minimization. SIAM review **52**(3), 471–501 (2010)

[24] Schmid, P.J.: Dynamic mode decomposition of numerical and experimental data. Journal of Fluid Mechanics **656**, 5–28 (2010)

[25] Taylor, G., Green, A.: Large ones. Proceedings of the Royal Society of London. Series A, Mathematical and Physical Sciences **158**(895), 499–521 (1937)

[26] Tu, J.H., Rowley, C.W., Luchtenburg, D.M., Brunton, S.L., Kutz, J.N.: On dynamic mode decomposition: Theory and applications. Journal of Computational Dynamics **1**(2), 391–421 (2014)

[27] Williams, M.O., Kevrekidis, I., Rowley, C.: A data–driven approximation of the koopman operator: Extending dynamic mode decomposition. Journal of Nonlinear Science **25**(6), 1307–1346 (2015)

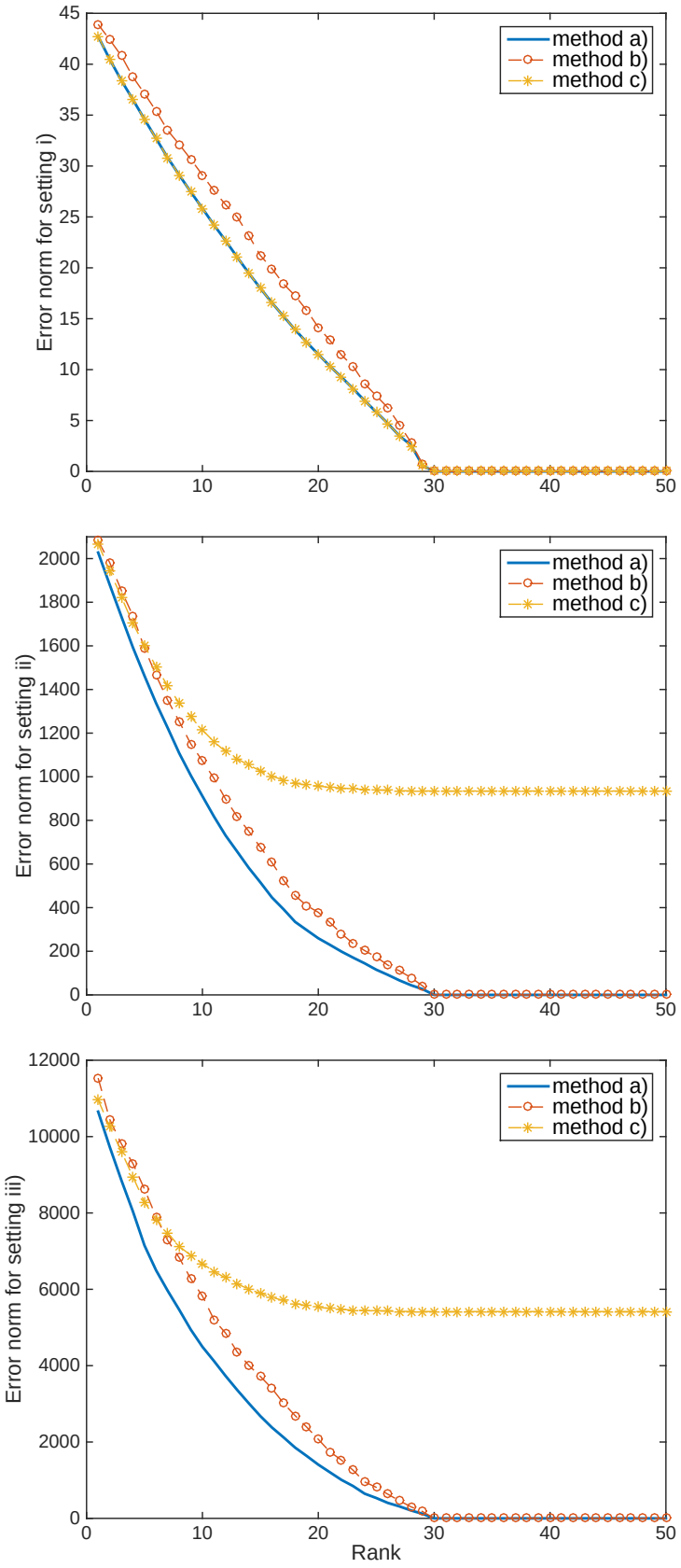

FIG. 5.1. *Evaluation of error norms* $\|\mathbf{X}' - \hat{A}_k\mathbf{X}\|_F$ *as a function of rank* k *for setting* i*),* ii*) and* iii*) and for methods* a*),* b*) and* c*). See details in Section 5.*

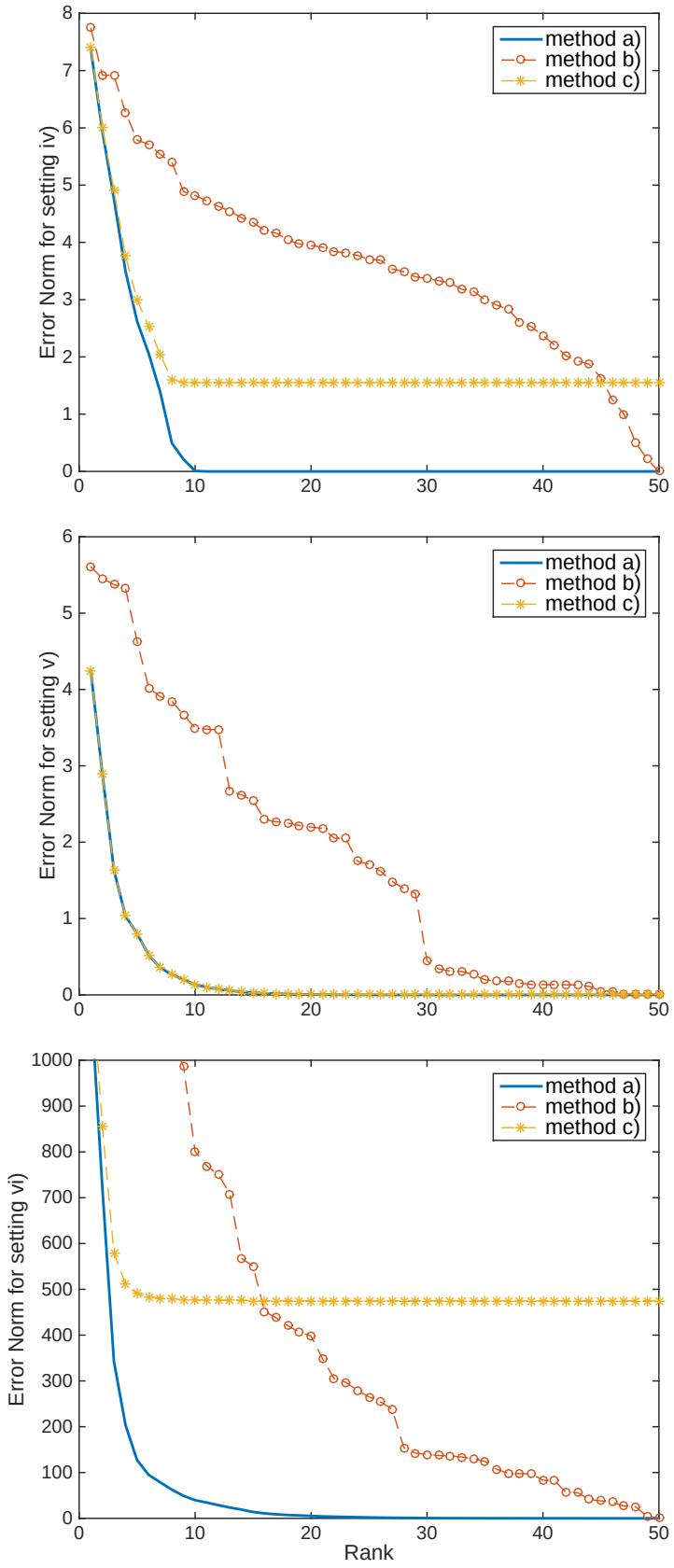

FIG. 5.2. *Evaluation of error norms* $\|\mathbf{X}' - \hat{A}_k\mathbf{X}\|_F$ *as a function of rank* k *for setting iv), v) and vi) and for methods a), b) and c). See details in Section 5.*

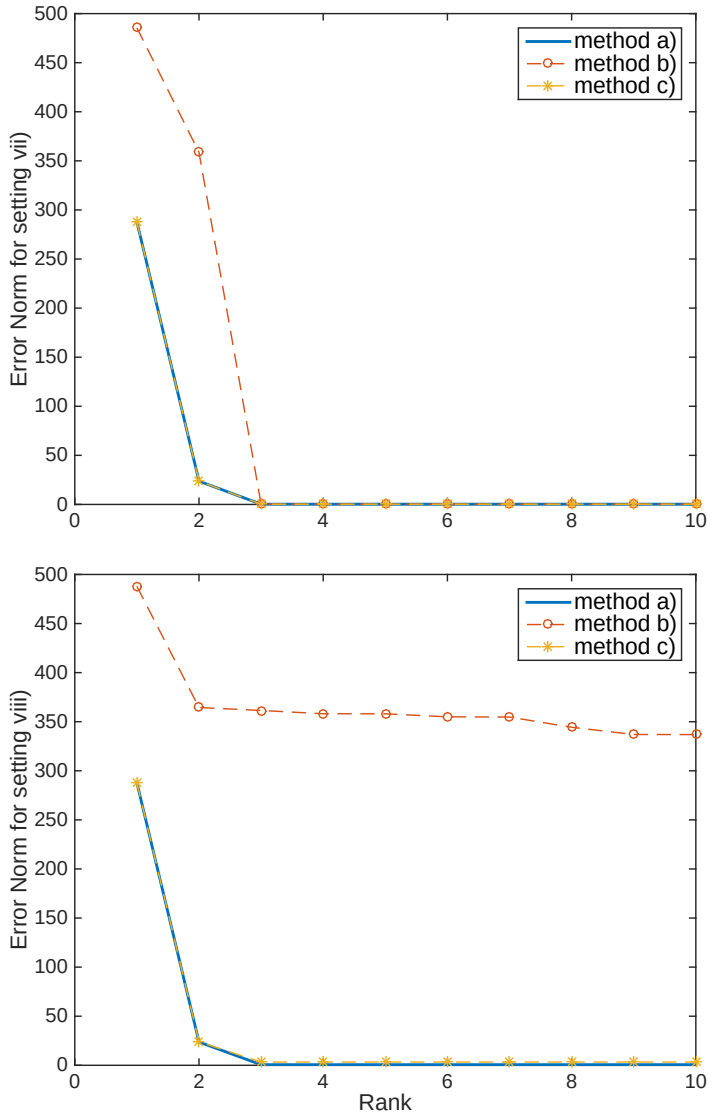

FIG. 5.3. *Evaluation of error norms* $\|\mathbf{X}' - \hat{A}_k\mathbf{X}\|_F$ *as a function of rank* k *for setting vii) and vii) and for methods a), b) and c). See details in Section 5.*

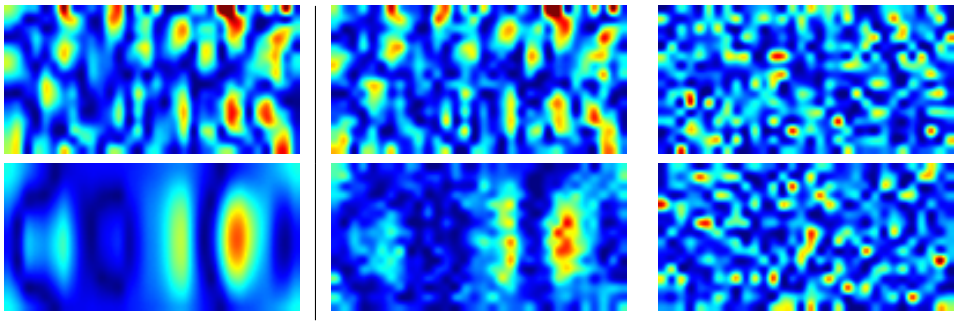

FIG. 5.4. *Extraction of DMD modes. Amplitude of the* 3*-rd DMD mode related to temperature (above) and buoyancy (below) in a Rayleigh-Bénard convective system. Reconstruction with method a) in the case of the noiseless setting vii) (left) and of the noisy setting viii) (middle). Reconstruction with method b) in the case of the noisy setting viii) (right).*